

Analyzing spectral peak distribution of coupled signals using Fourier transform theory

W Wenbing and Y Xiaojian*

School of Big Data, Fuzhou University of International Studies and Trade, Fuzhou, China

Received: 15 November 2022 / Accepted: 30 March 2023 / Published online: 23 May 2023

Abstract: Higher-order cumulants have a greater ability to mechanically reduce the impact of Gaussian noise, whether it is white or colored. As a consequence, higher-order statistical cumulants are gaining more attention in signal processing. Bispectral peaks arise due to phase coupling, and the distribution of these spectral peaks follows a special law. To analyze the distribution of these spectral peaks, this study adopted the method of harmonic decomposition. Based on Fourier transform theory, the harmonic frequencies where phase coupling occurs are calculated. By conducting a third-order cumulant analysis of the harmonics, the position of the spectral peak can be obtained. Then, using trigonometric functions, the methods of amplifying, reducing, and increasing the spectral peaks were discussed and verified through experiments. Since the collected vibration signal can be regarded as a function that satisfies the Fourier transform conditions, the above theoretical analysis can be applied to the analysis of various actual collected signals. Currently, bispectrum is generally used in actual applications to distinguish signal states by showing different peaks of the signal in different states. However, this application often encounters situations where the bispectrum in different states is difficult to distinguish. The experimental results showed that the methods of amplifying, reducing, and increasing the spectral peaks were helpful in strengthening the practical application effects of the bispectrum.

Keywords: Third-order cumulants; Phase coupling; Bispectral peaks; Distribution

1. Introduction

A random process can be completely described by its moments. Similarly, cumulants can be used to describe the statistical characteristics of random processes in the time domain. Higher-order spectra, including power spectra, can also be used to describe the statistical characteristics of random processes in the frequency domain. Higher-order spectra have many advantages compared to power spectra. Mainly, they can be used to check the “Gaussianness” of the process [1]. Because the third- and second-order spectra are always equal to zero, a higher-order spectrum can be used to check the Gaussian nature of the process. In addition, the third-order spectrum and the fourth-order cumulant spectrum can be used to filter out the zero-mean Gaussian distribution mixed in the signal. Higher-order spectra are also not sensitive to noise [2] and can detect the

nonlinearity of the system. Like the Gaussian process, the third-order spectrum of a sine signal is also equal to zero.

Under the excitation of a sine signal, the response of a steady-state linear system will still be a sinusoidal signal with the same frequency. However, the response to the input sine signal of a nonlinear system will contain higher-order harmonics, so the third-order spectrum is not equal to zero. For zero-mean white-noise excitation, the response of a linear system will not contain the contribution of higher-order transfer function, and the response and input will be independent of each other. However, for nonlinear systems, due to nonlinear effects, the response will contain the contribution of higher-order transfer functions, so the cumulant spectrum is not equal to zero [3]. Collis [4] proposed an approximate explanation for the physical meaning of the bispectrum and trispectrum. The phase of a non-Gaussian process can be estimated using higher-order spectra, which is important in long-distance communication and geophysics where non-minimum phase estimation of reflected waves and seismic wavelets needs to be solved.

Generally speaking, higher-order spectra can solve problems that power spectra cannot solve. When the phase

*Corresponding author, E-mail: yxj@fzfu.edu.cn

information is as important as, or even more important than, the amplitude information, the correlation-domain method can only accurately describe the minimum phase signal that is equivalent to the power-spectrum domain but cannot provide the correct phase information. Higher-order spectra are utilized to solve the non-minimum phase-channel equalization phase problem in communication. In the field of control systems, higher-order spectra are employed to identify system zeros and classify nonlinear systems.

The Gaussian process with higher-order spectra equal to zero indicates that higher-order cumulants as mathematical tools can theoretically completely suppress the influences of Gaussian noise. However, higher-order moments do not have this advantage because the moments of Gaussian processes with higher-order are not always zero. Therefore, in practical engineering applications, higher-order spectra as well as cumulant spectra are usually used as significant analysis tools for analyzing non-Gaussian random processes [5, 6]. The unclear physical meaning of higher-order spectra is one of the reasons why it is not widely used like power spectra. Power spectra characterize the distribution of signal energy with frequency, while the bispectrum and trispectrum have no clear physical meaning. Correlation analysis and Fourier transform can completely describe the second-order characteristics of a signal and are effective tools for processing Gaussian signals. Higher-order statistics are extensions of second-order statistics and include information that cannot be reflected by the correlation function and its Fourier transform results. For non-Gaussian signals, higher-order statistics reflect the degree to which the signal deviates from the Gaussian distribution.

Currently, bispectrum has been applied to fault diagnosis [7–9], radar signal analysis [10, 11], optical signal analysis [12], and astronomy [13, 14], among other fields. These applications use existing bispectrum theory to analyze the characteristics of bispectra of different signals and draw meaningful conclusions. In recent years, bispectrum analysis based on autoregressive models has also made new progress and obtained meaningful results [15–18]. The major contributions are explained as follows:

- The paper presents a comprehensive analysis of bispectral peaks and their formation due to phase coupling in signals.
- The paper proposes a method of harmonic decomposition to analyze the distribution of spectral peaks and, using Fourier transform theory, calculates the harmonic frequencies where phase coupling occurs.
- The paper conducts a third-order cumulant analysis of the harmonics to obtain the position of the spectral peak and discusses methods of amplifying, reducing, and

increasing the spectral peaks using trigonometric functions.

- The paper verifies the proposed methods through experiments and shows that they can effectively strengthen the practical application effects of bispectrum.
- The paper demonstrates the applicability of the theoretical analysis to various actual collected signals.

However, none of the above-mentioned research and application documents seem to clearly explain the reasons for bispectral peaks and how the positions and sizes of these peaks are determined. Additionally, none of them attempted to change the bispectral peak distribution in existing theories. The formation of bispectral peaks is due to the phenomenon of phase coupling in the signal, and the bispectral peak is the embodiment of this phase coupling. This study will comprehensively discuss the reasons for the formation of bispectral peaks and propose several methods to change the distribution of bispectral peaks in actual signals. The remaining sections of the paper are organized as follows: Various surveys are elucidated in Sect. 2, the proposed methodology is described in Sect. 3, the experimental results are described in Sect. 4, and the conclusion is described in Sect. 5.

2. Literature survey

Czeliński et al. [18] carried out a high-order spectral evaluation to accurately detect structural damages using nonlinear vibro-acoustic methods. They analyzed and predicted the severities of damages using amplitude and phase coupling processes and examined response data using bicoherence and bispectrum of modulation signals. However, this approach resulted in some computational complexities.

Guo et al. [19] introduced an average filter-based modulated signal bispectrum (EAVG-MSB) to retain impulse feature information without degrading their characteristics by harmonics and background noises. However, the efficiency of the EAVG filter was limited by the length of the structural element, so the length was adaptively optimized utilizing the maximum kurtosis index. The EAVG-MSB technique generated optimal results in extracting negative and positive impulse features, but had difficulty analyzing modulated signals.

Zandvoort and Nolte [20] jointly introduced recommendations to deal with high-frequency amplitudes by enhancing cross-entropy coupling measures to eliminate misinterpretations. The coupling process is influenced when cross-frequency and phase amplitude correlation is measured using phase amplitude coupling. Smearing

estimation results were mitigated using diverse filter settings, but this generates difficulties in distinguishing wide-band phenomena from high harmonics.

Guo et al. [21] developed an auto-regression model-based modulation signal bispectrum (AR-MSB) method for machinery fault detection and Gaussian noise reduction. Parameters such as amplitude, frequency, and probability density were applied to determine the performance rate. The experimental results showed a high accuracy rate in fault feature extraction. However, the AR-MSB method is not suitable to detect faults with variable speed conditions.

Huang et al. [22] investigated conventional bispectrum (CB) and modulation signal bispectrum (MSB) for monitoring motor-driven systems. They characterized sideband-based simulated signals to discuss the proficiency of MSB and the inefficiency of CB. The current signals were analyzed using both CB and MSB methods, and performance metrics such as amplitude and frequency were used for experimental purposes to measure several rotor faults, such as different compressor faults, downstream gearbox wear progression, and broken rotor bar (BRB).

Saidi et al. [23] discussed identifying the permanent magnet synchronous generator (PMSG) by utilizing stator current bispectrum analysis. They used the bispectrum to construct more precise diagnostic designs. The experimental results demonstrated that the scheme was highly effective but failed to acquire cost-efficient blade condition.

Guo et al. [24] presented modulation signal bispectrum (MSB) for extracting the modulation signature by suppressing random noise. They authenticated the multistage noise minimization approach using simulation investigation. The simulation displays that the MSB scheme achieved higher accuracy but failed to be regarded as an accurate and efficient technique for fault feature extraction.

Wang et al. [25] evaluated the sparse modulation signal bispectrum (MSB) analysis approach to acquire fault frequencies by the rolling bearing. The sparse MSB (S-MSB) was more appropriate for investigating the complex modulated signal. The diagonal slice was performed for acquiring the MSB sparse representation, which enhanced the efficiency and eliminated the harmonic frequency. However, the S-MSB approach did not eliminate the harmonic frequency interference.

3. Proposed methodology

Bispectral peaks arise due to phase coupling, and the distribution of these spectral peaks follows a special law. To analyze the distribution of these spectral peaks, this study adopted the method of harmonic decomposition. A detailed

explanation of formation of bispectral peaks due to phase coupling in the harmonics is discussed in the following subsections.

3.1. Coupled signals

Let $x(n)$ be the random signal:

$$x(n) = \sum_{i=1}^6 A_i \cos(\omega_i n + \phi_i) \quad (1)$$

where $\omega_2 > \omega_1 > 0$, $\omega_3 = \omega_1 + \omega_2$, $\omega_5 > \omega_4 > 0$, $\omega_6 = \omega_4 + \omega_5$, $\phi_6 = \phi_4 + \phi_5$. Here, $\phi_1, \phi_2, \dots, \phi_5$ is an independent random variable uniformly distributed on $(0, 2\pi)$ and then w_4, w_5, w_6 is called the coupled harmonic component.

Since Fourier transform of cosine signal is:

$$\begin{aligned} \cos \omega_i t &\leftrightarrow \frac{1}{2} [2\pi\delta(\omega - \omega_i) + 2\pi\delta(\omega + \omega_i)] \\ &= \pi\delta(\omega + \omega_i) + \pi\delta(\omega - \omega_i) \end{aligned} \quad (2)$$

$$\sin \omega_i t \leftrightarrow -j\pi\delta(\omega - \omega_i) + j\pi\delta(\omega + \omega_i) \quad (3)$$

get:

$$\begin{aligned} X(n) = \cos(\omega_i t + \phi_i) &\leftrightarrow \pi \cos \phi_i [\delta(\omega + \omega_i) + \delta(\omega - \omega_i)] \\ &- j\pi \sin \phi_i [\delta(\omega + \omega_i) - \delta(\omega - \omega_i)] = X(\omega) \end{aligned} \quad (4)$$

Therefore, for the coupled signal given by Eq. (1), the Fourier transform cannot distinguish the phase relationship of $\phi_6 = \phi_4 + \phi_5$. This is because for the Fourier spectrum, there will be spectral peaks on w_1, w_2, \dots, w_6 , and the role of $\phi_1, \phi_2, \dots, \phi_6$ are only to change the size of these peaks.

3.2. Recognition of coupled signals by bispectrum

This section provides the detailed description of the recognition of coupled signals by bispectrum. Here, the bispectral peak analysis is carried out on deterministic sequence, random process and analog signals. These steps are discussed as follows.

3.2.1. Bispectral peak analysis of deterministic sequence

Let $\{x(n)\}$ be a deterministic sequence, then its bispectral definition is

$$B_x(\omega_1, \omega_2) = X(\omega_1)X(\omega_2)X^*(\omega_1 + \omega_2) \quad (5)$$

If $x(t) = A + \cos \omega_o t$,
then

$$X(\omega) = A\delta(\omega) + \frac{1}{2}\pi[\delta(\omega + \omega_o) + \delta(\omega - \omega_o)] \quad (6)$$

Substituting Eq. (6) into Eq. (5) gives

$$B_x(\omega_1, \omega_2) = \begin{cases} A^3(\omega_1, \omega_2) = (0, 0) \\ \frac{A}{4}(\omega_1, \omega_2) = (\pm\omega_0, 0), (0, \pm\omega_0), (-\omega_0, \omega_0), (\omega_0, \omega_0) \\ 0 \text{ otherwise} \end{cases} \quad (7)$$

The bispectrum of $x(t)$ is shown in Fig. 1.

3.2.2. Bispectral peak analysis of random process

The random signal $\{x(n)\}$ containing zero-mean value provides the third-order cumulant of process as [6]:

$$c(k, l) = E[x(n)x(n+k)x(n+1)] \quad (8)$$

Substituting Eq. (1) into $[x(n)x(n+k)x(n+1)]$, it can be observed that the multiplication term consists of three columns, each of which has six terms, and the multiplication result has a total of 216 terms. Parameters A_i, ω_i, ϕ_i in the first column are represented by $A_i^f, \omega_i^f, \phi_i^f$; s the second column is represented by $A_i^s, \omega_i^s, \phi_i^s$; the third column is represented by $A_i^t, \omega_i^t, \phi_i^t$; then, its product general term can be found.

After expanding, we get

$$\begin{aligned} & A_i^f A_i^s A_i^t \cos[\omega_i^f n + \phi_i^f] \cos[\omega_i^s(n+k) + \phi_i^s] \cos[\omega_i^t(n+l) + \phi_i^t] \\ &= \frac{1}{4} A_i^f A_i^s A_i^t \{ \cos[\omega_i^f n + \omega_i^s(n+k) + \omega_i^t(n+l) + \phi_i^f + \\ & \quad \phi_i^s + \phi_i^t] + \cos[\omega_i^f n \\ & \quad + \omega_i^s(n+k) - \omega_i^t(n+l) + \phi_i^f + \phi_i^s - \phi_i^t] \\ & \quad + \cos[\omega_i^f n - \omega_i^s(n+k) + \omega_i^t(n+l) \\ & \quad + \phi_i^f - \phi_i^s + \phi_i^t] + \cos[\omega_i^f n - \\ & \quad \omega_i^s(n+k) - \omega_i^t(n+l) + \phi_i^f - \phi_i^s - \phi_i^t] \} \end{aligned} \quad (9)$$

Let $\phi_i^f = \phi_4, \phi_i^s = \phi_5, \phi_i^t = \phi_6$, and consider a cosine term in (9), for instance,

$$\cos[\omega_i^f n + \omega_i^s(n+k) - \omega_i^t(n+l) + \phi_i^f - \phi_i^s - \phi_i^t]$$

To make

$$E \left\{ \cos[\omega_i^f n + \omega_i^s(n+k) - \omega_i^t(n+l) + \phi_i^f + \phi_i^s - \phi_i^t] \right\} / = 0 \quad (10)$$

then $\phi_i^f + \phi_i^s - \phi_i^t = 0$ is needed.

In (10), if $\phi_i^f = \phi_4 - \phi_i^s = \phi_5, \phi_i^t = \phi_6$, then

$$\begin{aligned} E \left\{ \cos[\omega_i^f n + \omega_i^s(n+k) - \omega_i^t(n+l) + \phi_i^f + \phi_i^s - \phi_i^t] \right\} \\ = \cos(\omega_{05}k - \omega_{06}l) \end{aligned} \quad (11)$$

For the same reason, if

$$\phi_i^f = \phi_4 - \phi_i^s = \phi_5, \phi_i^t = \phi_6$$

then

$$\begin{aligned} E \left\{ \cos[\omega_i^f n + \omega_i^s(n+k) - \omega_i^t(n+l) + \phi_i^f + \phi_i^s - \phi_i^t] \right\} \\ = \cos(\omega_{04}k - \omega_{06}l) \end{aligned} \quad (12)$$

According to the above method, we get

$$\begin{aligned} c(k, l) = \frac{A_4 A_5 A_6}{4} [\cos(\omega_{05}k + \omega_{04}l) + \cos(\omega_{06}k - \omega_{04}l)] \\ + \cos(\omega_{04}k + \omega_{05}l) \\ + \cos(\omega_{06}k - \omega_{05}l) + \cos(\omega_{04}k - \omega_{06}l) \\ + \cos(\omega_{05}k - \omega_{06}l) \end{aligned} \quad (13)$$

For terms of the form $\cos(\omega_{01}k + \omega_{02}l)$, to investigate the distribution of its bispectral peaks, we must substitute it into the following bispectral expression:

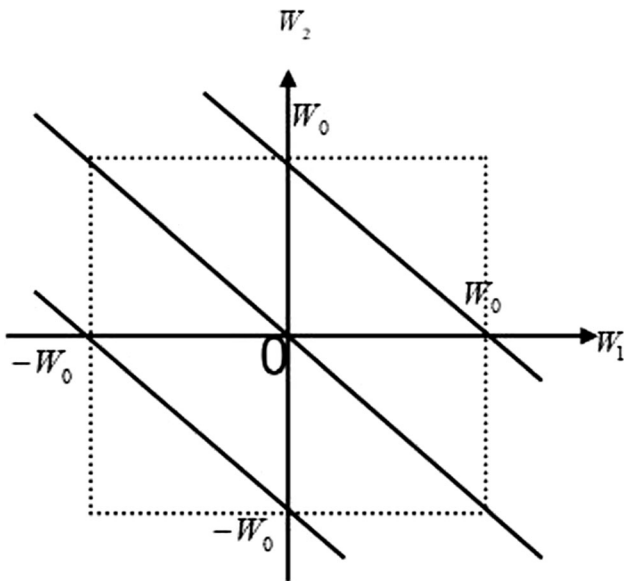


Fig. 1 Cosine signal bispectrogram

$$S_{3,x}(\omega_1, \omega_2) = \sum_{k=-\infty}^{\infty} \sum_{l=-\infty}^{\infty} C_{3,x}(k, l) \exp[-j(\omega_1 k + \omega_2 l)] \quad (14)$$

According to the Fourier transform result obtained by cosine function in Eq. (2), it is inferred that the bispectrum of the operation result contains the following product terms:

$$[\delta(\omega_1 + \omega_{04}) + \delta(\omega_1 - \omega_{04})] * [\delta(\omega_2 - \omega_{05}) + \delta(\omega_2 - \omega_{05})] \quad (15)$$

So, for terms of the form $\cos(\omega_{01}k + \omega_{02}l)$, the non-zero points (spectral peaks) in the bispectrum include: $[(-\omega_{01}, -\omega_{02}), (-\omega_{01}, -\omega_{02}), (\omega_{01}, -\omega_{02}), (\omega_{01}, \omega_{02})]$.

It can be seen that only the harmonics with phase coupling can produce spectral peaks in the bispectrogram, and the spectral peaks appear at the intersection of the frequencies of the two harmonics with phase coupling.

3.2.3. Spectrum peak analysis of analog signals

According to the $x(n)$ in Eq. (1), the following random signal was generated:

$$y = \cos(4\pi x + a1) + \cos(6\pi x + a2) + \cos(10\pi x + a3) + \cos(30\pi x + a4) + \cos(50\pi x + a5) + \cos(80\pi x + a6) \quad (16)$$

Among them, $a1, a2, \dots, a6$ were independent random variables uniformly distributed on $(0, 2\pi)$ and $a6 = a5 + a4$. The bispectrum image is shown in Fig. 2.

Figure 2 displays there were apparent peaks at the frequencies (15, 25) and (25, 15). This result was consistent with the theoretical analysis.

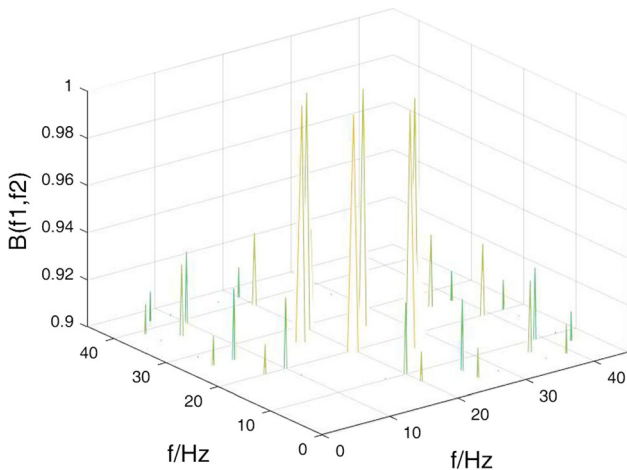


Fig. 2 Bispectrum of analog signal

3.2.4. Specific calculation method of bispectral coupling signal

According to the Fourier transform theorem, a function $f(t)$ with T as the period satisfies the Dirichlet condition in the interval $[-\frac{T}{2}, \frac{T}{2}]$:

1. Discontinuities with finite number;
2. Extreme points with finite number. Then, it can be developed into a Fourier series. At consecutive points:

$$f(t) = a_0 + \sum_{n=1}^{\infty} (a_n \cos n\omega t + b_n \sin n\omega t) \quad (17)$$

where $\omega = \frac{2\pi}{T}$,

$$a_n = \frac{2}{T} \int_{-\frac{T}{2}}^{\frac{T}{2}} f(t) \cos n\omega t dt, (n = 0, 1, 2, \dots) \quad (18)$$

$$b_n = \frac{2}{T} \int_{-\frac{T}{2}}^{\frac{T}{2}} f(t) \sin n\omega t dt, (n = 0, 1, 2, 3, \dots) \quad (19)$$

Based on Euler's formula:

$$e^{j\theta} = \cos \theta + j \sin \theta \quad (20)$$

Equation (17) turns into

$$f(t) = c_0 + \sum_{n=1}^{\infty} c_n \cos(n\omega_1 t + \varphi_n) \quad (21)$$

where

$$c_n^2 = a_n^2 + b_n^2, \varphi_n = \arctan\left(-\frac{b_n}{a_n}\right), c_0 = a_0 \quad (22)$$

If the phase coupling condition is to be satisfied, then

$$\varphi_k = \varphi_i + \varphi_j \quad (23)$$

must be satisfied, such that

$$\arctan\left(-\frac{b_k}{a_k}\right) = \arctan\left(-\frac{b_i}{a_i}\right) + \arctan\left(-\frac{b_j}{a_j}\right) \quad (24)$$

4. Results and discussion

For attaining the operating signals from t pressure-reducing valves, the experiments are conducted in two states such as normal and fault. The further investigations are explained in the next subsections.

4.1. Data collection

The experimental results were simulated using a pilot-operated pressure-minimizing valve. The normal working operation of pressure minimization valve is affected when there exists a foreign matter in the outlet and inlet ports of

valves. To achieve operating signal of pressure-minimizing valves in faulty as well as normal states, the following criteria are made.

Normal state: It represents working condition of pressure-reducing valve in normal state.

Fault state: φ 3 mm iron core is included to the inlet as well as outlet ports of pressure-minimizing valve.

In this experiment, pressure-reducing valve's operating signal was collected for two fault states and the normal operation state of each of the 18 acquisition groups of 54 sets of data. The maximum number of data used by this experimentation was 1024.

4.2. Mechanical signal verification of coupled signal phase

According to the method in 4.1, select a set of data collected by the pressure-reducing valve in usual working conditions, decompose this set of data according to the Fourier transform method, then follow the methods in Eqs. (18) and (19), calculate the coefficients a_n and b_n , then calculate the corresponding phase φ_n , then get a corresponding phase array, hence find the array elements that satisfy the phase coupling relationship $\varphi_k = \varphi_i + \varphi_j$ in this array according to the requirements of Eq. (24), and record their corresponding subscripts; then, these subscripts are the frequencies corresponding to these harmonics, and the harmonic frequency that meets the phase coupling condition obtained by the calculation result is [2 86 298, 32 216 428, 65 179 222, 65 292 335, 74 87 144, 74 370 427, 74 454 466, 86 216 482, 87 370 440, 179 292 449, 261 300 453, 283 483 489, 287 299 485, 296 357 0], a total of 14 groups.

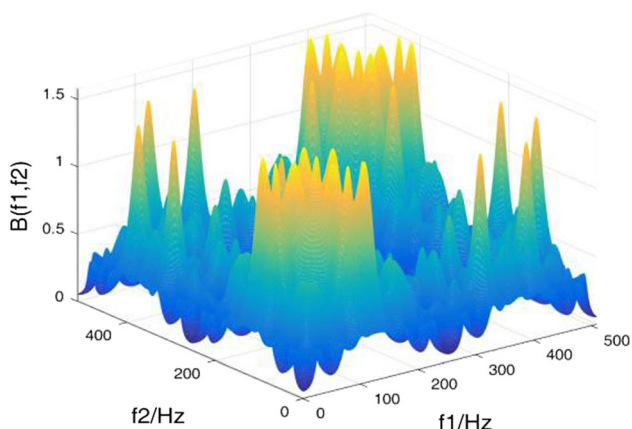


Fig. 3 The bispectrum of the group

Then, according to formula (14), the bispectrum of this group of data (displayed in Fig. 3) reveals that, regardless of the symmetry of the bispectrum, there are about 13 bispectrum peaks in this set of data, which are roughly the same as the 14 harmonics that meet the phase coupling conditions calculated earlier, which illustrates the previous analysis in this article is correct. From the results obtained, as long as the phase coupling condition of $\varphi_k = \varphi_i + \varphi_j$ is met, spectral peaks can be generated in the bispectrogram, regardless of whether the frequency of the corresponding harmonic satisfies the sum-difference relationship of $\omega_k = \omega_i + \omega_j$. Take the first element (74 87 144) in the value as an example, the first component 2 represents the frequency ω_i in the harmonic $\cos(\omega_i n + \phi_i)$, the second represents $b \omega_j$ in the harmonic $\cos(\omega_j n + \phi_j)$, and the third represents ω_k in the harmonic $\cos(\omega_k n + \phi_k)$. It can be seen that $\omega_i + \omega_j$ is not equal to ω_k , but the phases of the three harmonic components satisfy the condition $\varphi_k = \varphi_i + \varphi_j$.

Therefore, in Fig. 3, there is a bispectral peak at the coordinates (74, 87). From the calculation results, the harmonics of the same frequency can also form a phase coupling relationship with the harmonics of different frequencies at the same time. For example, a harmonic with a frequency of 74 Hz can be combined with (74 87 144), (74 370 427) and (74 454 466), these three groups of harmonics of different frequencies form a phase coupling relationship, and this phenomenon is reflected in the bispectrogram as there are multiple spectral peaks on a certain straight line. In the experiment process, when the calculation accuracy of Eq. (24) is determined to retain two decimal digits, the number of groups of harmonic frequencies that meet the phase coupling condition is almost infinite; when it is determined to be three decimal places, the number of groups is in hundreds of groups and nearly 1000 groups; when it is determined to be four digits after the decimal point, the number of groups is in dozens of groups and nearly 100 groups; when it is determined to be five digits after the decimal point, the number of groups is the aforementioned 14 groups; when it is further determined that it is six digits after the decimal point, there is no answer. This situation shows that the solution of Eq. (24) is related to the calculation accuracy, but it raises a question, that is, what is the theoretical solution of Eq. (24). It can be seen from Eq. (24) that this equation is an underdetermined equation, that is, an equation contains three unknowns, and theoretically, there should be infinite solutions.

From the above analysis, it can be concluded that the peaks of the bispectrum are generated by the phase coupling phenomenon, and this phase coupling is a real phenomenon. Therefore, bispectrum can objectively reflect the

phase coupling phenomenon existing in real signals and is an effective signal analysis method.

4.3. Amplification method of bispectral peaks

For a deterministic signal, after differentiation, its bispectrum is approximately equal to

$$B_x^1 = \omega_i^3 X(\omega_1)X(\omega_2)X^*(\omega_1 + \omega_2) \quad (25)$$

After it is differentiated n times, the corresponding bispectrum becomes

$$B_x^n = \omega_i^{3n} X(\omega_1)X(\omega_2)X^*(\omega_1 + \omega_2) \quad (26)$$

For a random signal, after differentiating $x(n)$ in Eq. (1), it can be substituted into Eq. (13) to obtain

$$c(k, l) = \frac{A_4 A_5 A_6 \omega_{04} \omega_{05} \omega_{06}}{4} [\cos(\omega_{05}k + \omega_{04}l) + \cos(\omega_{06}k - \omega_{04}l) + \cos(\omega_{04}k + \omega_{05}l) + \cos(\omega_{06}k - \omega_{05}l) + \cos(\omega_{04}k - \omega_{06}l) + \cos(\omega_{05}k - \omega_{06}l)] \quad (27)$$

After differentiation n times, we get

$$c(k, l) = \frac{A_4 A_5 A_6 \omega_{04}^n \omega_{05}^n \omega_{06}^n}{4} [\cos(\omega_{05}k + \omega_{04}l) + \cos(\omega_{06}k - \omega_{04}l) + \cos(\omega_{04}k + \omega_{05}l) + \cos(\omega_{06}k - \omega_{05}l) + \cos(\omega_{04}k - \omega_{06}l) + \cos(\omega_{05}k - \omega_{06}l)] \quad (28)$$

From Eqs. (25) to (28), it can be seen that through the differentiation method, whether deterministic or random signals, the spectral peaks of the coupled harmonics can be highlighted. Additionally, as the order of differentiation increases, if the product of the three frequencies $\omega_{04}\omega_{05}\omega_{06}$ in the coupled harmonics is larger, the peaks of the spectrum are more and more prominent.

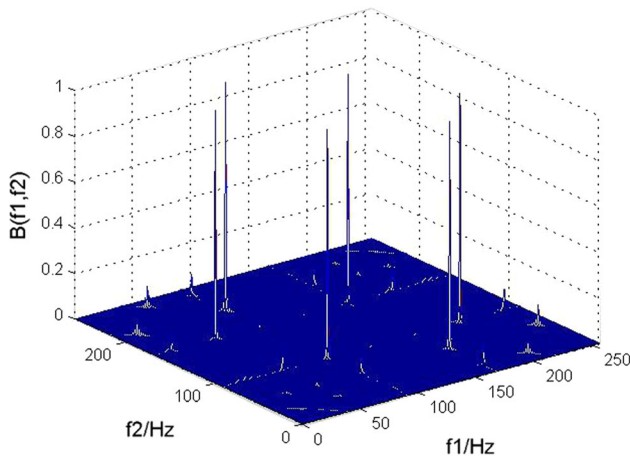


Fig. 4 The bispectrum in the normal state

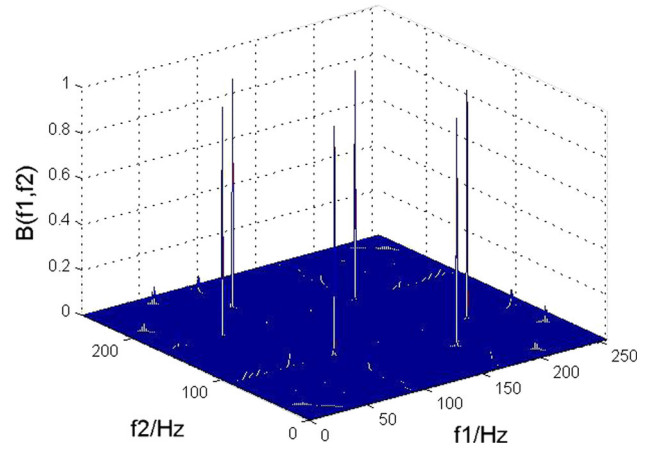


Fig. 5 The bispectrum in the fault state

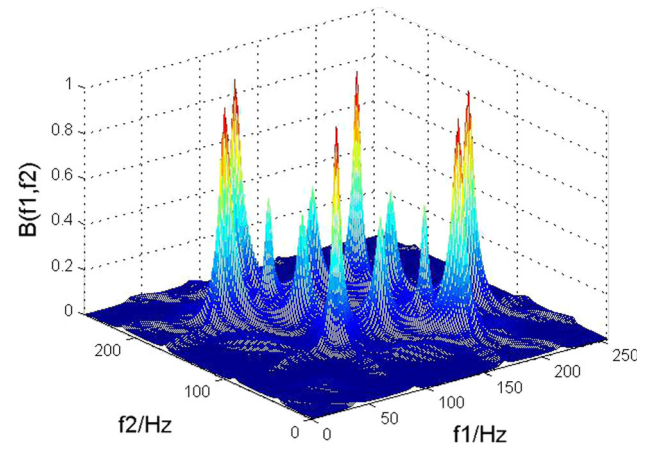


Fig. 6 The bispectrum in the normal state after differentiation

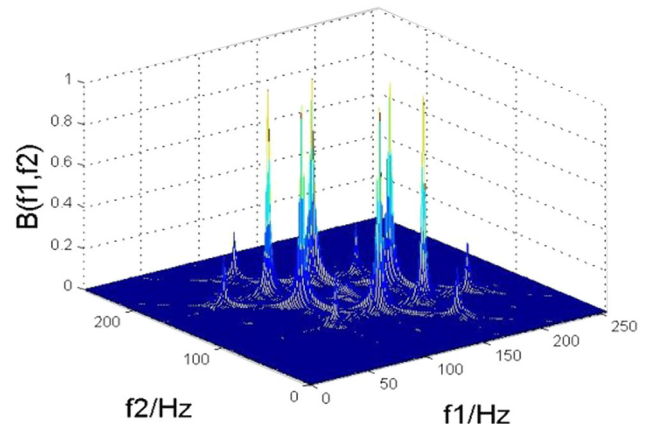


Fig. 7 The bispectrum in the fault state after differentiation

Figures 4 and 5 show the bispectra of the two sets of signals in normal and fault states. As can be seen from the figure, they were very similar. Figures 6 and 7 show the bispectra corresponding to the data of Figs. 4 and 5 after

being differentiated once. It can be seen that the difference between Figs. 6 and 7 became more obvious. Under normal conditions, once differentiated, the spectral peaks became thicker and more numerous, and although similar changes occurred in the data of the fault state, the degree of change was smaller.

4.4. Method of adding bispectral peaks

For $x(n)$ in Eq. (1): $x(n) = \sum_{i=1}^6 A_i \cos(\omega_i n + \phi_i)$,
let

$$x(n) = \sum_{i=1}^6 (i=1) A_i \cos(\omega_i n + \phi_i) \tag{29}$$

where $\phi_3 \neq \phi_1 + \phi_2$, so the phase coupling condition is not met.

Consider

$$\begin{aligned} (\cos \alpha + \cos \beta)^2 &= \cos^2 \alpha + 2 \cos \alpha \cos \beta + \cos^2 \beta \\ &= 1 + \frac{1}{2}(\cos 2\alpha + \cos 2\beta) \\ &\quad + (\cos(\alpha + \beta) + \cos(\alpha - \beta)) \end{aligned} \tag{30}$$

Since there is a $\cos(\alpha + \beta)$ term in Eq. (29), let $\alpha = \omega_1 n + \phi_1$, $\beta = \omega_2 n + \phi_2$.

Then,

$$\cos(\alpha + \beta) = \cos((\omega_1 + \omega_2)n + \phi_1 + \phi_2) \tag{31}$$

It can be seen from Eq. (31) that through the square-sum operation, the required coupling components are artificially generated by two harmonic components that do not originally have phase coupling: $(\omega_1 + \omega_2)n + \phi_1 + \phi_2$.

Therefore, for Eq. (29), let $y(n) = x_1(n) + x_1^2(n)$, then $y(n)$ must also contain the harmonic components of at the same $\omega_1 n + \phi_1$, $\omega_2 n + \phi_2$, $(\omega_1 + \omega_2)n + \phi_1 + \phi_2$ time, meaning that a signal that meets the phase coupling condition is artificially generated.

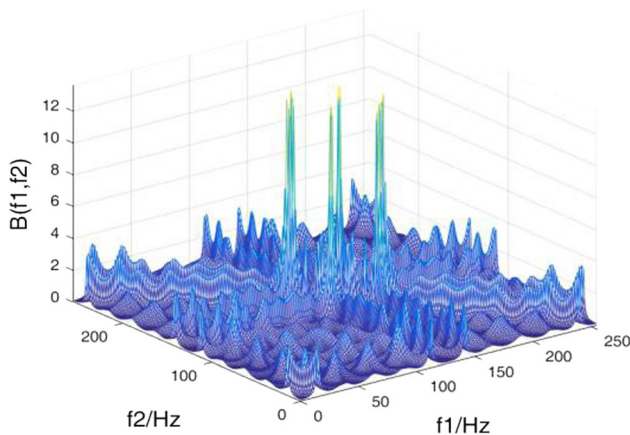


Fig. 8 The bispectrum in the normal state

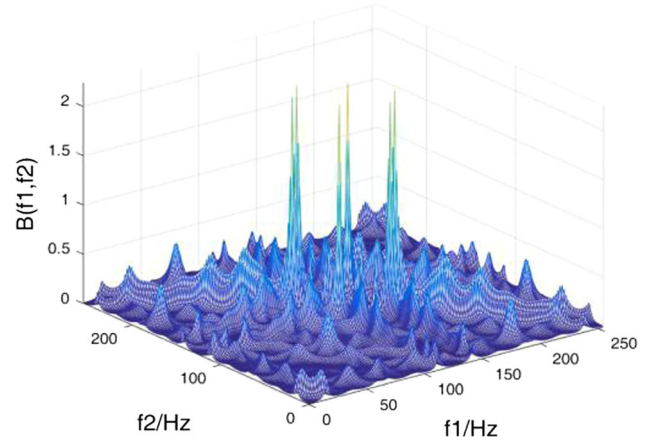


Fig. 9 The bispectrum in the fault state

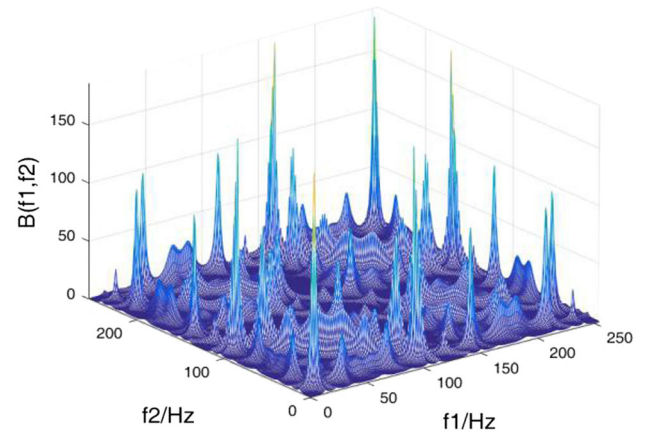


Fig. 10 The bispectrum in the normal state after peaks added

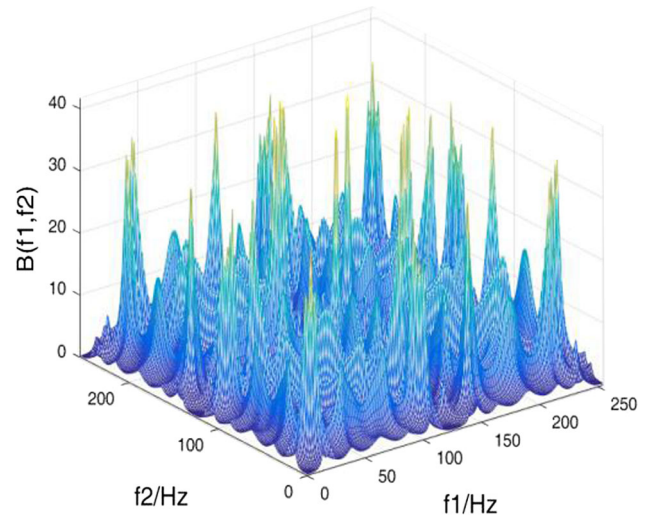


Fig. 11 The bispectrum in the fault state after peaks added

Observe the following formula:

$$\begin{aligned}
 &(\cos \alpha + \cos \beta + \cos \gamma)^2 \\
 &= \frac{3}{2} + \frac{1}{2}(\cos 2\alpha + \cos 2\beta + \cos 2\gamma) + \cos(\alpha + \beta) \\
 &+ (\cos(\alpha - \beta) + \cos(\alpha + \gamma) + \cos(\alpha - \gamma)) + \cos(\beta + \gamma) + \cos(\beta - \gamma)
 \end{aligned} \tag{32}$$

Here,

$$x_2(n) = \sum_{i=1}^6 A_i \cos(\omega_i n + \phi_i) \tag{33}$$

where $\varphi_6 = \varphi_4 + \varphi_5$ satisfies the phase coupling condition. Then, let $\alpha = \omega_4 n + \varphi_4, \beta = \omega_5 n + \varphi_5, \gamma = \omega_6 n + \varphi_6$

By substituting into Eq. (31), it can be seen that the harmonic components originally met the phase coupling condition. After the square-sum calculation, in addition to this term, $\cos(\alpha + \beta)$ the terms are added. After $\cos(\alpha + \gamma), \cos(\beta + \gamma)$ operation of square sum, not only is the previous coupling term retained, but some new coupling terms are added. That is, the square-sum operation can increase the number of bispectral peaks of the original signal.

Here, two diverse sets of data were chosen, in which one is utilized for normal state and the other is for fault state. It can be seen from Figs. 8 and 9 that the bispectra were very similar and difficult to distinguish. Assuming that the original data were represented by $x(n)$, after $y(n) = x(n) + x^2(n)$, the bispectrum of the signal $y(n)$ was calculated. The corresponding outcomes of two data sets are displayed in Figs. 10 and 11. It can be seen that, compared with Figs. 8 and 9, in Figs. 10 and 11, the bispectral peaks of the two sets of data were significantly increased, making it possible to distinguish the two mechanical operating states that were difficult to distinguish by bispectra alone. Since the number of peaks in Fig. 10 is significantly more than that in Fig. 11 after the

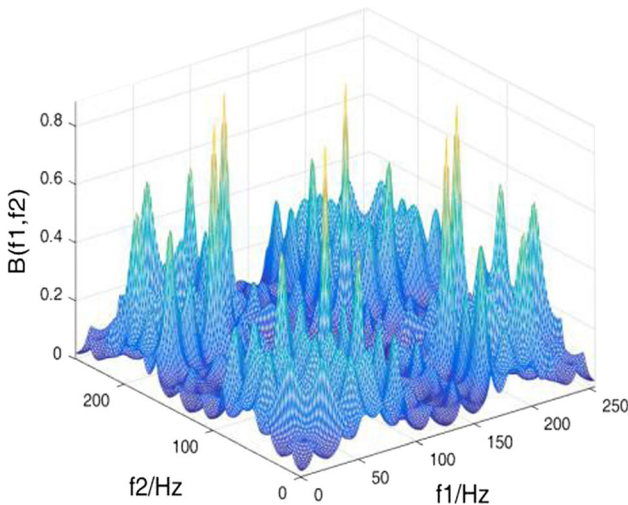


Fig. 12 The bispectrum in the normal state

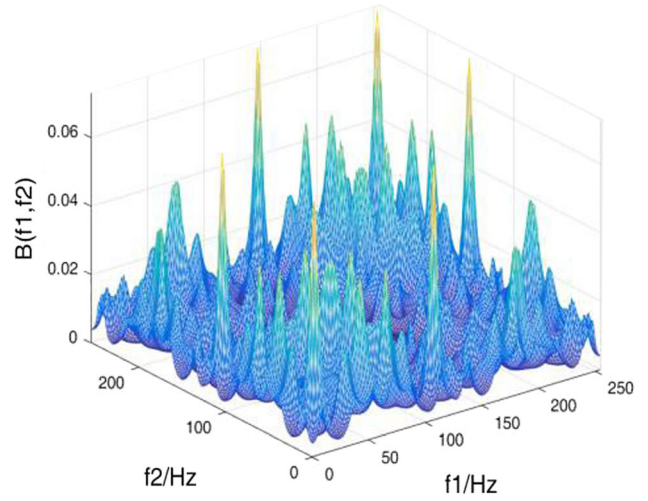


Fig. 13 The bispectrum in the fault state

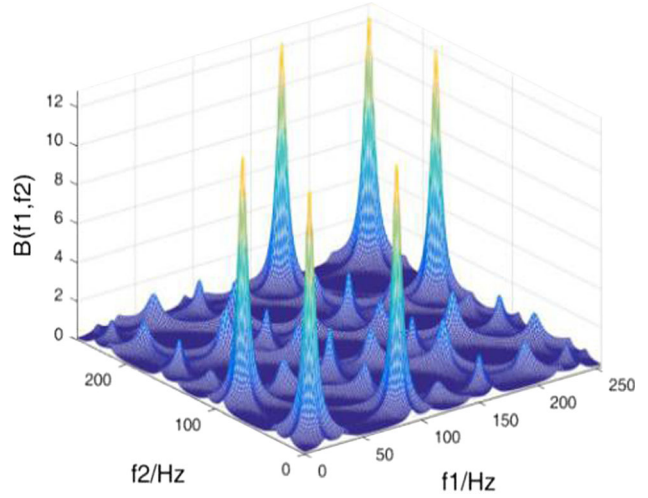


Fig. 14 The bispectrum in the normal state after peaks added

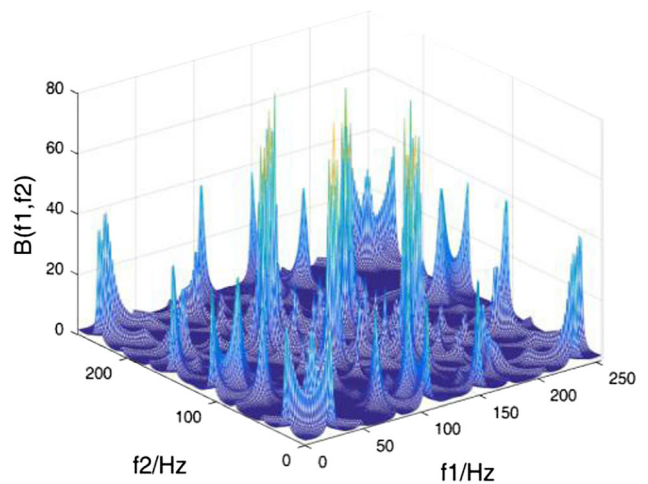


Fig. 15 The bispectrum in the fault state after peaks added

square-sum calculation, this phenomenon further illustrates that the square-sum calculation can make the harmonic components that do not meet the phase coupling conditions match. Presumably, the original signal in the fault state contains more harmonic components that do not meet the phase coupling conditions than the corresponding components of the original signal in the normal state.

4.5. Method of suppressing bispectral peaks

Set: $x_2(n) = \sum_{i=1}^6 A_i \cos(\omega_i n + \phi_i)$, where $\phi_6 \neq \phi_4 + \phi_5$ meet the phase coupling condition, and let $\alpha = \omega_4 n + \phi_4, \beta = \omega_5 n + \phi_5, \gamma = \omega_6 n + \phi_6$

Consider the following equations:

$$\begin{aligned} & \cos((\omega_4 n + \phi_4) + \cos(\omega_4 n + \phi_4)) \\ & = 2 \cos(\omega_4 n + (\phi_4 + \phi_4)/2) \cos(((\phi_4 - \phi_4)/2)) \quad (34) \end{aligned}$$

$$\begin{aligned} & \cos((\omega_5 n + \phi_5) + \cos(\omega_5 n + \phi_5)) \\ & = 2 \cos(\omega_5 n + (\phi_5 + \phi_5)/2) \cos(((\phi_5 - \phi_5)/2)) \quad (35) \end{aligned}$$

Among them, ϕ_4, ϕ_5 can be any value in the interval $[0, 2\pi]$, and $\cos(\omega_4 n + \phi_4)$, $\cos(\omega_5 n + \phi_5)$ are signal components that are added artificially.

The $\phi_6 \neq \phi_4 + \phi_5$ equation that originally satisfies the phase coupling relationship is changed into $\phi_6 \neq (\phi_4 + \phi_4 + \phi_5 + \phi_5)/2$, which no longer meets the phase coupling condition.

To conduct experimental verification, in a similar fashion to the previous section, a set of data was also taken in normal and fault states, and bispectra are shown in Figs. 12 and 13. To determine the frequency of the added signal, an algorithm was adopted. The normal state and fault state of bispectrum after adding peaks are described in Figs. 14 and 15.

The algorithm to determine the frequency of the added signal is given as follows:

1. Calculate the bispectrum of the signal to be added.
2. Determine a number of spectral peaks from large to small in the bispectral results obtained, and record the frequency coordinates of each spectral peak at the same time.
3. The determined frequency-coordinate value is used as the frequency of the added cosine signal, and the phase of the signal can be randomly generated.

According to the above algorithm, in the experiment, five values were taken from large to small according to the size of the peak of the spectrum, and then, the corresponding cosine signals were constructed. These were then added to the original signal in Figs. 12 and 13, and the corresponding bispectra were obtained, as shown in Figs. 14 and 15. Compared with Figs. 12 and 13, the peaks of Figs. 14 and 15 were significantly reduced. It can also be

seen from Figs. 14 and 15 that although Figs. 12 and 13 are difficult to distinguish, after taking the above measures to suppress the peaks, the composition of the peaks in Fig. 14 was obviously simpler than that in Fig. 15. The peaks in Fig. 13 were also relatively more concentrated. This shows that the components of the fault-state signal may be more complicated than that of the normal-state signal. At the same time, by adopting the above method, the bispectral peaks of the signal could be successfully reduced. This also shows that the coupled harmonic component $\cos(\omega_6 n + \phi_6)$ in the mechanical signals could possibly exist independently of its constituent components $\cos(\omega_4 n + \phi_4)$, $\cos(\omega_5 n + \phi_5)$. Otherwise, this method of reducing the bispectral peaks would not succeed.

5. Conclusions

Bispectrum analysis has gained significant attention in various fields such as mechanical fault diagnosis, radar signal analysis, and sound signal analysis, among others. The formation of bispectral peaks is due to phase coupling in harmonics, which can be utilized to distinguish signal states. However, in some cases, bispectrum in different states can be difficult to distinguish, and thus, methods to enhance the application result of bispectrum have been proposed. This study analyzed the generation mechanism of coupled harmonic signals for bispectral peaks and proposed a method to calculate the number of bispectral peaks and their positions. The proposed methods to amplify, increase, and suppress bispectral peaks can make bispectra more distinguishable for signals that were originally indistinguishable. Experimental testing confirmed the effectiveness of the proposed methods, which may make bispectrum more applicable in practical engineering situations. By using these methods, the distribution of bispectral peaks in different states can be changed, making it easier to distinguish between different states. The results of this study contribute to the development of bispectrum analysis and provide a new perspective for studying the distribution of bispectral peaks. Furthermore, the proposed methods offer practical solutions for enhancing the application efficiency of bispectrum analysis in various fields. In summary, this study contributes to the understanding of bispectrum analysis and its potential applications in mechanical fault diagnosis, radar signal analysis, and sound signal analysis. The proposed methods provide practical solutions for improving the application efficiency of bispectrum analysis and may lead to new developments in this area.

Acknowledgements This paper was supported by the Research Start-up Fund for high-level talents of FuZhou University of International

Studies and Trade (FWKQJ202006) and 2022 Guiding Project of Fujian Science and Technology Department (2022H0026).

Authors' contributions WW agreed on the content of the study and methodology. WW and YX collected all the data for analysis and completed the analysis based on agreed steps. The results and conclusions were discussed and written together. The author read and approved the final manuscript.

Funding Not applicable.

Availability of data and material Data sharing is not applicable to this article as no new data were created or analyzed in this study.

Code availability Not applicable.

Declarations

Conflict of interest The authors declare that they have no conflict of interest.

Consent to participate Not applicable.

Consent for publication Not applicable.

Human and animal rights This article does not contain any studies with human or animal subjects performed by any of the authors.

Informed consent Informed consent was obtained from all individual participants included in the study.

References

- [1] J Guo, Z Shi, D Zhen, Z Meng, F Gu and AD Ball *Structural Health Monitoring* **21** 984 (2022)
- [2] J Newman, A Pidde and A Stefanovska *Applied and Computational Harmonic Analysis* **51** 171 (2021)
- [3] I Abroug and N Abcha, A Jarno and F Marin *Natural Hazards and Earth System Sciences* **20** 3279 (2020)
- [4] L Saidi, M Benbouzid, D Diallo, Y Amirat, E Elbouchikhi and T Wang *Energies* **13** 2888 (2020)
- [5] M Xu, Y Han, X Sun, Y Shao, F Gu and AD Ball *Mechanical Systems and Signal Processing* **165** 108280 (2022)
- [6] V G Böning, A C Birch, L Gizon, TL Duvall and J Schou *Astronomy & Astrophysics* **635** A181 (2020)
- [7] X Pang, X Xue and W Jiang *IEEE/ASME Transactions on Mechatronics* **99** 1 (2020)
- [8] M Sohaib and J Kim *IEEE Transactions on Instrumentation and Measurement* **99** 1 (2019)
- [9] J Guo, Z Shi and H Li *Sensors* **18** 2908 (2018)
- [10] D Xie, KS Chen and X Yang *IEEE Journal of Selected Topics in Applied Earth Observations and Remote Sensing* **99** 1 (2019)
- [11] R Cao, J Cao and JP Mei *Multimedia Tools and Applications* (2018)
- [12] J Ren, JG Lv and BX Zhao *IEEE Access* **99** 1 (2021)
- [13] B Pope, L Pueyo and Y Xin *The Astrophysical Journal* **907** 40 (2021)
- [14] G Harker, S Cole and A Jenkins *Monthly Notices of the Royal Astronomical Society* **382** 1503 (2018)
- [15] Y Han, M Xu, X Sun, X Ding X Chen and F Gu *IEEE Sensors Journal* **22** 4400 (2022)
- [16] A Martín-Montero et al. *Entropy* **23** 1016 (2021)
- [17] Z Li, J Jiao, Y Wu, R Xie and Z Wang *In International Conference on Intelligent Automation and Soft Computing* 1283 (2021)
- [18] K Czeluśniak, WJ Staszewski and F Aymerich *Mechanical Systems and Signal Processing* **178** 109199 (2022)
- [19] J Guo, D Zhen, H Li, Z Shi F Gu and AD Ball *ISA transactions* **101** 408 (2020)
- [20] CS Zandvoort and G Nolte *Journal of Neuroscience Methods* **350** 109032 (2021)
- [21] J Guo, H Zhang, D Zhen, Z Shi, F Gu and A.D Ball *Measurement* **151** 107240 (2020)
- [22] B Huang, G Feng, X Tang, J X Gu, G Xu, R Cattley *Energies* **12** 1438 (2019)
- [23] L Saidi, M Benbouzid, D Diallo, Y Amirat, E Elbouchikhi and T Wang *In IECON 2019–45th Annual Conference of the IEEE Industrial Electronics Society* 1 6998 (2019)
- [24] J Guo, D Zhen, H Li, Z Shi, F Gu and AD Ball *Measurement* **139** 226 (2019)
- [25] G Wang, F Gu, I Rehab, A Ball and L Li *Mathematical Problems in Engineering* (2018)

Publisher's Note Springer Nature remains neutral with regard to jurisdictional claims in published maps and institutional affiliations.

Springer Nature or its licensor (e.g. a society or other partner) holds exclusive rights to this article under a publishing agreement with the author(s) or other rightsholder(s); author self-archiving of the accepted manuscript version of this article is solely governed by the terms of such publishing agreement and applicable law.